Studies of rubber-toughened poly(methyl methacrylate): 1. Preparation and thermal properties of blends of poly(methyl methacrylate) with multiple-layer toughening particles

P. A. Lovell*, J. McDonald, D. E. J. Saunders and R. J. Young
Polymer Science and Technology Group, Manchester Materials Science Centre, UMIST, Grosvenor Street, Manchester M1 7HS, UK
(Received 9 March 1992)

The use of sequential emulsion polymerization to prepare toughening particles which comprise two, three and four radially alternating rubbery and glassy layers is described. The conditions which lead to control of particle size and morphology are discussed. The particles were crosslinked during their formation in order to ensure that they retained their size and morphology during blending with poly(methyl methacrylate) (PMMA). In this way, rubber-toughened (RT) PMMA materials with rubbery phases of predefined particle size and morphology were produced, as confirmed by transmission electron microscopy. The glass transitions of the three types of RTPMMA materials were essentially identical because the matrix PMMA was common to each blend and because the rubbery and glassy phases of each of the types of toughening particle were identical in composition.

(Keywords: poly(methyl methacrylate); thermal properties; blends)

INTRODUCTION

Poly(methyl methacrylate) (PMMA) is a classic example of a brittle thermoplastic and for several decades efforts have been made to improve its fracture resistance via rubber toughening[1,2]. The earlier efforts focused upon use of suspension polymerization to produce composite beads consisting of both PMMA and rubbery phases[3]. Although these materials were commercialized, they were deficient in that the morphology, and hence toughness, of artefacts produced from them was very strongly dependent upon the moulding conditions employed. There was, therefore, great scope for improvement and, in particular, a need to develop rubber-toughened (RT) PMMA materials the toughness of which could be more reproducibly controlled and would be less susceptible to the processing regime. During the last two decades these improvements have been achieved by blending the matrix PMMA with separately prepared toughening particles[4]. Emulsion polymerization is used to prepare the toughening particles which typically comprise two to four radially alternating rubbery and glassy layers, the outer layer always being of glassy polymer. The particles are crosslinked during their formation in order to ensure that they retain their morphology and size during blending with PMMA and during subsequent moulding of the blends. This route to RTPMMA has the distinct advantage of allowing independent control of the properties of the matrix PMMA, the composition, morphology, size of the dispersed rubbery phase and the level of inclusion of the toughening particles. Although these improved materials have been commercialized successfully, in comparison to other toughened polymers there are relatively few reports of investigations into their preparation, properties and deformation behaviour. This paper is the first in a series based upon a major research programme aimed at elucidating the mechanism(s) of toughening, and optimizing toughness, in these materials. The preparation and thermal properties of materials containing two-, three- and four-layer toughening particles are described and discussed critically. The stress–strain and fracture properties of these materials will be the subject of the second paper in the series.

EXPERIMENTAL

Materials

Potassium persulphate (BDH AnalaR, >99%) and Aerosol OT (Cyanamid) were used as supplied. Distilled water was deionized (Elgacan C114) to a conductivity $<0.2\ \mathrm{mS\ cm^{-1}}$ prior to use. Methyl methacrylate (MMA), ethyl acrylate (EA), n-butyl acrylate (BA), styrene (S) and allyl methacrylate (ALMA) (polymerization grade monomers, Aldrich, ≥99%) were used as supplied for the $9\ \mathrm{dm^3}$ preparations of toughening particles. However, for the smaller-scale preparations used to study reaction kinetics, the monomers were treated several times with dilute sodium hydroxide solution to remove phenolic inhibitors, washed thoroughly

*To whom correspondence should be addressed

0032-3861/93/010061-09

with water, dried and then distilled under nitrogen at reduced pressure before use.

Preparation of the toughening particles

The two-, three- and four-layer (i.e. 2L, 3L and 4L) toughening particles which are represented schematically in *Figure 1* were prepared by sequential emulsion polymerizations in which seed particles were first formed and then grown in either two or three stages. The base comonomer formulations used for the formation of the rubbery and glassy layers were BA–S (78.2:21.8 mol%) and MMA–EA (94.4:5.1 mol%), respectively. ALMA was included at specific, constant levels (in the range 0.1–3.0 mol%) in the comonomer formulations used to form the inner layers (i.e. all of the rubbery layers and the inner glassy layers), but was not added to the comonomer formulation used to form the outer glassy layers.

The polymerizations were performed at 80°C under a flowing nitrogen atmosphere on a scale $\sim 9\ dm^3$ in a $10\ dm^3$ flanged reaction vessel. For each of the preparations, seed particles of 0.10 μm diameter were formed first using the relative quantities of comonomer mixture and water given in *Table 1*. Aerosol OT was included in the seed-stage formulations at a level of 0.6 wt% of the comonomer mixture and the polymerization was initiated by addition of potassium persulphate such that its aqueous phase concentration was 0.5 mmol dm^{-3}. After 45 min (which was found to be sufficient for complete conversion of the seed-stage comonomers) the seed particles were grown in stages by sequential, metered additions of appropriate quantities of the comonomer mixtures together with synchronized concurrent additions of Aerosol OT at levels of 0.6 and 0.8 wt% for the formation of the rubbery and glassy layers, respectively. At ~ 1 h intervals during the growth stages, further additions of potassium persulphate were made to increment its aqueous phase concentration by ~ 0.4 mmol dm^{-3} each time. Upon completion of the addition of the comonomer mixture for a given growth stage, sufficient time was allowed for complete conversion of these monomers before beginning addition of the comonomer mixture for the next growth stage.

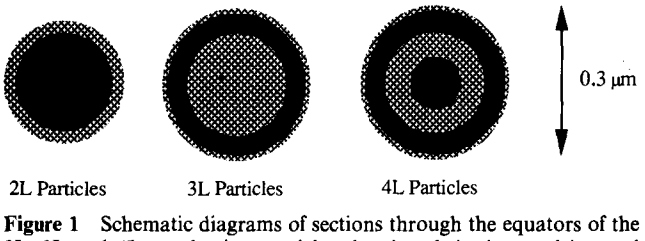

Figure 1 Schematic diagrams of sections through the equators of the 2L, 3L and 4L toughening particles showing their sizes and internal structures: rubbery layers are shown in black and glassy layers are cross-hatched

Table 1 Relative quantities of comonomer mixture and water used in the formulations for the seed stages

	Mass of comonomer mixture per unit volume of water (g dm^{-3})	
Seed stage for:	Rubbery seed	Glassy seed
2L particles	32.79	–
3L particles	–	23.42
4L particles	23.42	–

In the preparation of the 2L particles, the seed particles were grown first to a diameter of 0.19 μm by formation of rubbery polymer, and then to a diameter of 0.23 μm by formation of the outer glassy layer.

In the preparation of the 3L and 4L particles, the seed particles were grown first to a diameter of 0.20 μm by formation of glassy polymer, then to a diameter of 0.28 μm by formation of rubbery polymer, and finally to a diameter of 0.30 μm by formation of the outer glassy layer.

The formation of the desired particle morphologies was monitored by analysing aliquots removed from the reactions for the overall percentage monomer conversion (from gravimetric analysis for latex solids content) and for z-average particle diameter, D_z (from photon correlation spectroscopy performed on a Malvern Autosizer IIc using the method of cumulants analysis[5,6]).

For each type of toughening particle, the latex obtained from emulsion polymerization was coagulated by addition to magnesium sulphate solution to yield loose aggregates of the particles. These were isolated by filtration, washed thoroughly with water and then dried at 70°C. In each case, samples of the coagulum were assayed for magnesium by extraction with a boiling concentrated HNO_3/concentrated H_2SO_4 mixture, followed by analysis of the diluted extract for magnesium using a Pye-Unicam SP9 atomic absorption spectrophotometer. For all batches of toughening particles prepared, the level of magnesium was found to be <60 ppm.

Preparation of the blends

The dried aggregates of toughening particles were blended with the matrix PMMA (Diakon LG156, ex. ICI) at 220°C by either a single pass through a Werner–Pfleiderer 30 mm twin-screw extruder or two passes through a Francis–Shaw 40 mm single-screw extruder. For each type of particle, four blends containing different weight fractions, w_p, of particles were produced. The nomenclature used to define the blends is illustrated by 3L22 which specifies that the blend contains 3L particles with $w_p = 0.22$.

Characterization

G.p.c. was carried out using 0.2% (w/v) solutions in tetrahydrofuran (THF). Each solution (70 μl) was injected into the THF flowstream of a g.p.c. system operating at 30°C, and the polymer separated on a series of three columns of 10 μm PL gel with porosities of 500, 10^4 and 10^6 Å using a flow rate of $1\ cm^3\ min^{-1}$. Polystyrene standards (Polymer Laboratories) were used for calibration.

The morphologies of the materials were studied using a Philips 301 transmission electron microscope operated at 100 kV. Two types of specimen were examined: (1) thin films cast from dispersions containing 0.04–0.16 g dm^{-3} of toughening particles in a 40 g dm^{-3} solution of matrix PMMA in toluene; and (2) thin sections cut at room temperature from the bulk materials using a DuPont 5000 Ultramicrotome fitted with a diamond knife (ex. Gaetani).

D.s.c. was performed on a DuPont 990 thermal analyser equipped with a DuPont 910 DSC cell and cell base. Samples (~ 15 mg) contained in crimped aluminium pans were analysed over the temperature

range -100 to 160°C employing a nominal heating rate of 20°C min^{-1} and an empty crimped aluminium pan as the reference. Glass transition temperatures (T_gs) were located by the point of intersection of an extension of the baseline prior to the transition with a tangent drawn at the point of steepest slope in the baseline step, and for each material average values were obtained from analysis of three samples with a reproducibility of ± 2°C.

Specimens ($\sim 45 \times 9 \times 3$ mm) for dynamic mechanical thermal analysis (d.m.t.a.) were cut from 3 mm thick plaques prepared by compression moulding of the materials at 200°C. The dynamic mechanical measurements were made using a Polymer Laboratories DMTA with the specimen mounted in a double cantilever-beam head, and were recorded in the temperature range -100 to 160°C employing a heating rate of 5°C min^{-1} with an operating frequency of 1 Hz. For each material, three specimens were analysed and mean data for variation of the storage modulus, E', loss modulus, E'', and loss tangent, $\tan \delta$, with temperature were recorded. The T_g values were located from the peaks in $\tan \delta$ and were reproducible to ± 2°C.

RESULTS AND DISCUSSION

Design of the toughening particles

The design of the toughening particles takes into account a number of general requirements. Since many of the applications for RTPMMA materials demand a high percentage transmission of visible light (comparable to that of the matrix PMMA), it is essential to prevent light scattering by the dispersed toughening particles. This is achieved by selecting the compositions of the rubbery and glassy layers in the particles so that their refractive indices are equal to that of the matrix PMMA which has $n_D^{20} = 1.489$. Theoretical refractive indices for copolymers, n_{cop}, can be calculated using the following equation[7]:

$$n_{cop} = \sum_i w_i n_i \qquad (1)$$

in which w_i and n_i are, respectively, the weight fraction of repeat units in the copolymer and the refractive index of the homopolymer for comonomer i. By considering n_i values[8] together with monomer reactivity ratios for copolymerization[9] it is possible to identify a number of candidate copolymers. For the rubbery layers, these include poly[(n-butyl acrylate)-*co*-butadiene] (P-BA/B) comprising 46.9 wt% (67.7 mol%) B repeat units, poly[(n-butyl acrylate)-*co*-isoprene] (P-BA/I) comprising 41.8 wt% (57.5 mol%) I repeat units, and poly[(n-butyl acrylate)-*co*-styrene] (P-BA/S) comprising 18.3 wt% (21.6 mol%) S repeat units. An important factor in selecting the copolymer to be used is weathering resistance, since in many applications the RTPMMA materials are competing with polycarbonate and it is desirable to retain the better weathering characteristics of PMMA. The much lower level of unsaturation in P-BA/S is, therefore, a major advantage and is the principal reason for its use as the basis for the rubbery layers in the toughening particles reported here. The use of P-BA/S, however, is not without compromise since it has a higher T_g than either P-BA/B or P-BA/I, which naturally will lead to a higher temperature for the brittle–ductile transition. Nevertheless, in relation to the current uses of RTPMMA, this does not present a problem[10].

The choice of copolymer for the glassy layers is somewhat simpler, since any poly[(methyl methacrylate)-*co*-(alkyl acrylate)] with the appropriate composition could be used. Poly[(methyl methacrylate)-*co*-(ethyl acrylate)] comprising 5.1 wt% (5.1 mol%) EA repeat units has been used in this work because it represents a reasonable compromise in terms of maintaining a high T_g (for work-up and blending purposes) and a low water uptake (for good weathering performance of the RTPMMA materials).

For each of the different types of toughening particle it is essential to have an outer glassy layer. This has two purposes: (1) to prevent coalescence of primary particles during formation and drying of the coagulum produced from the latexes, thus enabling good dispersions of the primary particles to be produced upon blending of the coagulum with the matrix PMMA; and (2) to mix with the matrix PMMA thereby providing a means of stress transfer from the matrix to the particles in the RTPMMA materials.

Further important considerations in the design of the toughening particles are the need for grafting at interfaces in the particles and for crosslinking in each of the internal phases. Grafting at interfaces is required for purposes of stress transfer between the different layers in the particles and is commonly referred to as graftlinking[4]. Crosslinking is necessary in order to prevent loss of particle integrity (i.e. morphology and size) upon blending with matrix PMMA at 200–220°C. The outer glassy layer does not need to be crosslinked since it is graftlinked to the (crosslinked) rubbery layer around which it is formed. This has the advantage that mixing of the outer glassy layer with the matrix PMMA is made easier and more efficient than would be possible for an outer glassy layer which is both graftlinked and crosslinked. The patent literature[4] highlights the need to use monomers which contain at least two C=C bonds of very different reactivity in order to achieve graftlinking and emphasizes that monomers containing (as one of the types of C=C bond) one or more allylic C=C bonds are particularly efficient for this purpose. In the present work, ALMA has been used both for graftlinking and for crosslinking. The chemistry of homo- and copolymerization of ALMA is being investigated as part of the current research programme and the results from these studies will be reported in a separate paper[11].

Preparation of the toughening particles

Figures 2–4 show the variation of overall percentage conversion with time for preparations of the 2L, 3L and 4L toughening particles, respectively. The conversion curves highlight the stages in the formation of the toughening particles and clearly show that before commencing addition of the monomer mixture for a particular growth stage, complete conversion of the monomer mixture added in the preceding stage is achieved. This is generally desirable because copolymerization with residual monomer would (at least initially) result in the formation of copolymer with a T_g which is different to that of the copolymer which is designed to be formed, and is crucial in the formation of the outer glassy layer since a reduction in the T_g of this layer due to copolymerization of the MMA–EA monomer mixture with residual BA can cause problems

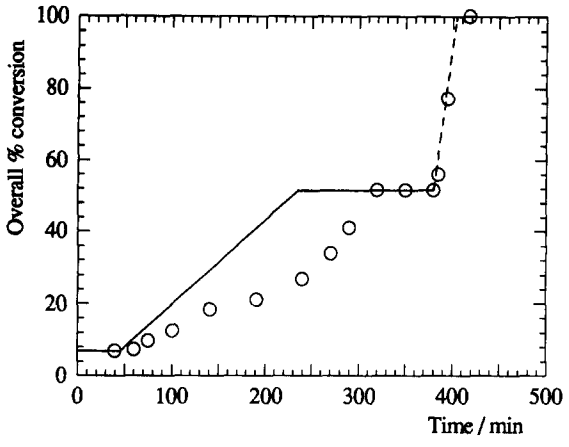

Figure 2 Variation of overall percentage conversion with reaction time for preparation of the 2L toughening particles. The solid and broken lines are the monomer feed profiles for the formation of rubbery and glassy layers, respectively

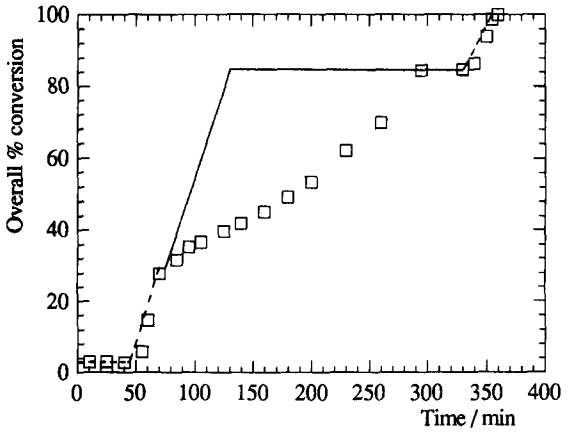

Figure 3 Variation of overall percentage conversion with reaction time for preparation of the 3L toughening particles. The solid and broken lines are the monomer feed profiles for the formation of rubbery and glassy layers, respectively

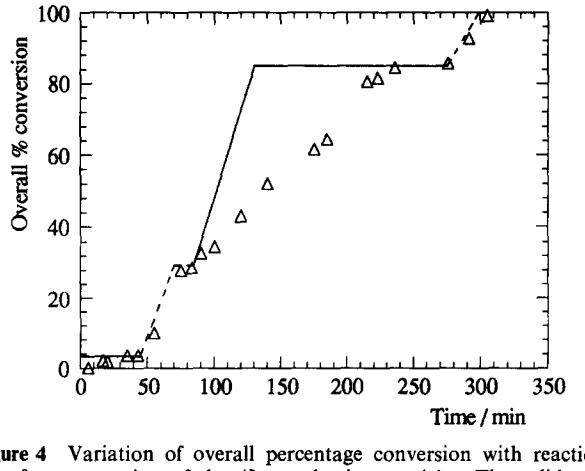

Figure 4 Variation of overall percentage conversion with reaction time for preparation of the 4L toughening particles. The solid and broken lines are the monomer feed profiles for the formation of rubbery and glassy layers, respectively

of particle coalescence during coagulation, work-up and drying of the particles.

Further inspection of the conversion curves reveals that the glassy layers are formed under monomer-starved conditions, whereas the rubbery layers form with monomer flooding[12]. On this basis, the glassy layers can be expected to have uniform composition, whereas the rubbery layers should comprise copolymer with a range of composition[13]. In order to obtain information on the composition drift in the formation of the rubbery layers, some of the aliquots removed during the rubbery layer growth stages in the 2L, 3L and 4L preparations were analysed for unreacted BA and S by gas–liquid chromatography. This enabled a mass balance approach to be used to calculate the average composition of the copolymer formed in particular intervals of conversion of these monomers. The results are plotted in *Figure 5* together with a theoretical curve for composition drift calculated using the 'terminal model' copolymer equation with values for monomer reactivity ratios ($r_{BA} = 0.164$ and $r_S = 0.698$) which were considered to be most reliable[14]. Use of other realistic published values of monomer reactivity ratios[9] slightly changes the position and shape of the theoretical curve but does not change the inferences drawn from comparison of the experimental and theoretical plots. The experimental data show the extent of composition drift and reveal that it largely follows the theoretical curve. Precise agreement cannot be expected in view of the effects of monomer partitioning between the aqueous phase, latex particles and (whilst they exist) monomer droplets. Initially, the deviation from theory is towards higher w_{BA}, suggesting that BA is preferentially absorbed into the latex particles. Although the differences in the solubility parameters of BA ($18.0\ J^{1/2}\ cm^{3/2}$)[15], S ($19.0\ J^{1/2}\ cm^{3/2}$)[15] and the glassy ($19.2\ J^{1/2}\ cm^{3/2}$)[16] and rubbery ($18.4\ J^{1/2}\ cm^{3/2}$)[16] copolymers are not sufficient to suggest major differences in miscibility, preferential absorption of BA may arise from favourable polar interactions of ester groups in BA with those in the acrylic repeat units of the copolymers.

The drift in copolymer composition during formation of the rubbery layers has been transposed into corresponding drifts in n_D^{20} and T_g assuming a linear dependence upon weight fraction composition[7,17] [i.e. equations of the form of equation (1)] and also, for T_g, using the Fox equation[18] (*Figures 6* and *7*). The calculations did not include contributions from the low level of ALMA present and were performed using the following values of n_D^{20} and T_g for the homopolymers[8,19]: (1) polystyrene, $n_D^{20} = 1.592$, $T_g = 100°C$; (2) poly(n-butyl acrylate), $n_D^{20} = 1.466$, $T_g = -54°C$. The deviation

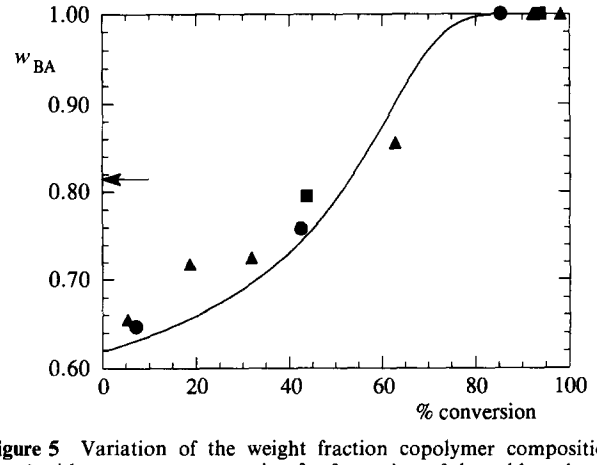

Figure 5 Variation of the weight fraction copolymer composition (w_{BA}) with percentage conversion for formation of the rubbery layers in the 2L (●), 3L (■) and 4L (▲) toughening particles. The solid line is the theoretical curve and the arrow indicates the mean copolymer composition (see text)

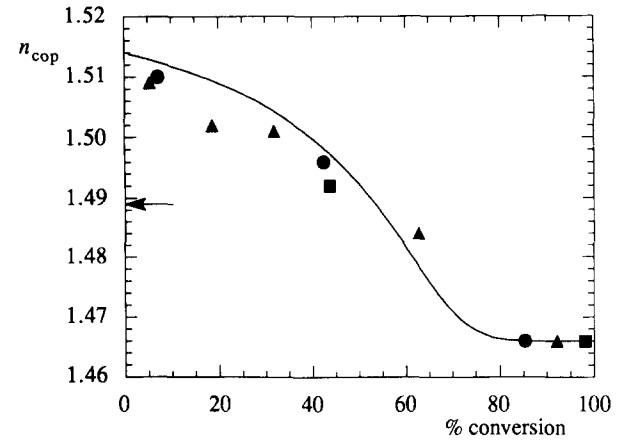

Figure 6 Variation of copolymer refractive index (n_{cop}) with percentage conversion for formation of the rubbery layers in the 2L (●), 3L (■) and 4L (▲) toughening particles. The solid line is the theoretical curve and the arrow indicates the mean copolymer refractive index (see text)

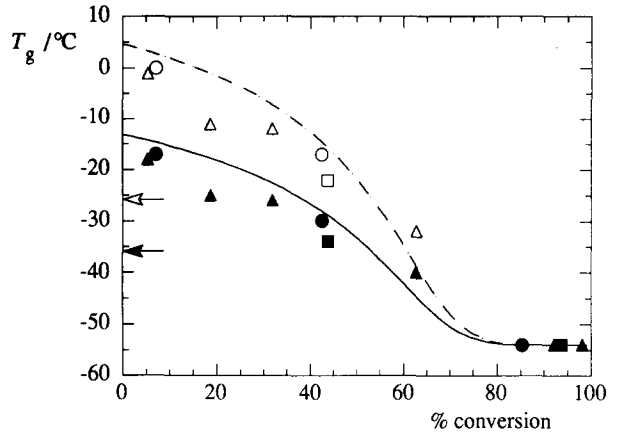

Figure 7 Variation of copolymer glass transition temperature (T_g) with percentage conversion for formation of the rubbery layers in the 2L (●, ○), 3L (■, □) and 4L (▲, △) toughening particles. The solid symbols and the solid theoretical line were calculated using the Fox equation; the open symbols and the broken theoretical line were calculated using a linear relationship between T_g and weight fraction composition (see text). The solid- and open-headed arrows indicate the corresponding mean theoretical values of the copolymer T_g

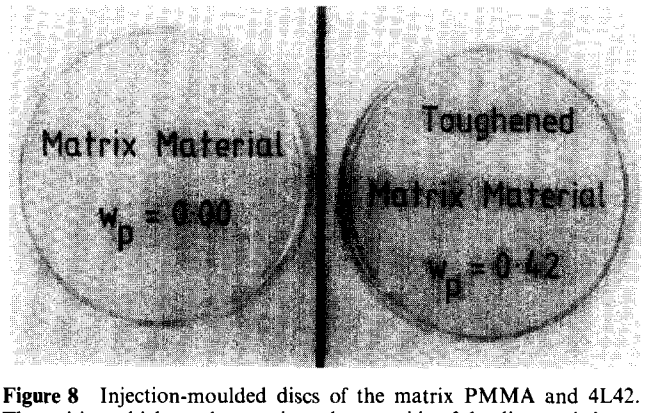

Figure 8 Injection-moulded discs of the matrix PMMA and 4L42. The writing which can be seen is at the rear side of the discs and shows visually that the two materials have similar optical transparencies

in refractive index from the target value of 1.489 is not serious with regard to loss of optical transparency, as can be seen from *Figure 8*. In commercial materials[20] prepared using essentially identical procedures to those described in this paper, there is ~2% loss in transmission for RTPMMA materials with $w_p = 0.42$. The implication of the drift in T_g is a broad transitional region for the rubbery phases. This is evident in the d.m.t.a. spectra which are discussed in the following section.

Attempts were made to eliminate the composition drift by reducing the rate of monomer addition[12,13]. However, even for very low rates of addition, this was not successful – there was always an initial period during which the rate of polymerization was low. The reason for the reduced rate of polymerization in the initial stages of formation of a rubbery layer is not completely clear. It may be related, in part, to the complete conversion of the monomers used in the preceding stage, since upon starting the addition of the monomer mixture for the next stage there is initially a requirement to swell the latex particles, at least at their surfaces, before polymerization and particle growth can take place. In this respect, the fact that there was no similar delay in the onset of polymerization in the formation of the glassy layers may be a consequence of higher rates of monomer diffusion arising from the much higher water solubilities, and hence aqueous phase concentrations, of MMA and EA as compared to those of BA and S[21]. A further indication of the origin of the reduced rate in the initial stages of S–BA copolymerization is provided by the observation that the lag in conversion is drastically reduced when S is omitted from the rubbery growth stage. Hence, a further factor that may be important is the ratio $k_p/k_t^{1/2}$ for homopolymerization, where k_p and k_t are, respectively, the rate constants for propagation and termination. The value of $k_p/k_t^{1/2}$ for S is approximately an order of magnitude smaller than for BA, MMA and EA[22]. Since S is preferentially consumed in copolymerization of the S–BA mixture, its lower value of $k_p/k_t^{1/2}$ will naturally lead to lower rates of copolymerization in the initial stages.

Figures 9–11 show the variation of D_z with time during formation of the 2L, 3L and 4L toughening particles, respectively. The theoretical curves were calculated from the percentage conversion data taking into account the densities of the rubbery (1.06 g cm^{-3}) and glassy (1.18 g cm^{-3}) polymers[23] and the measured diameters of the seed particles, and by assuming that (1) no new particles are formed after the seed stage and (2) the particles are not swollen by unreacted monomer. The good agreement between experimental and theoretical diameters for the particles at the end of each growth stage

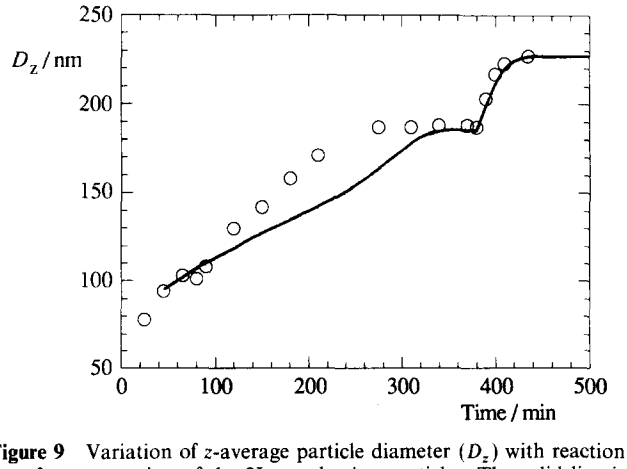

Figure 9 Variation of z-average particle diameter (D_z) with reaction time for preparation of the 2L toughening particles. The solid line is the theoretical curve (see text)

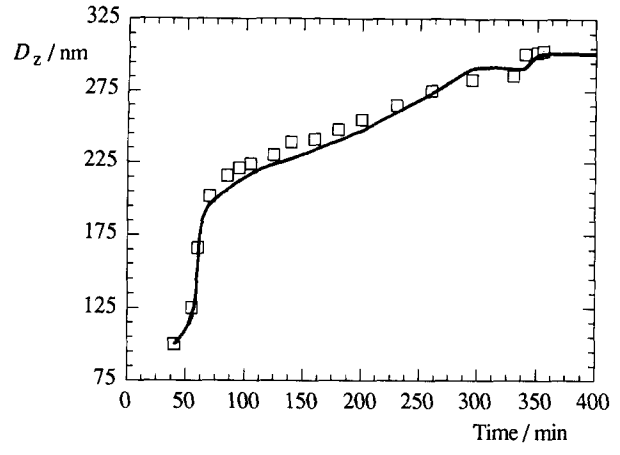

Figure 10 Variation of z-average particle diameter (D_z) with reaction time for preparation of the 3L toughening particles. The solid line is the theoretical curve (see text)

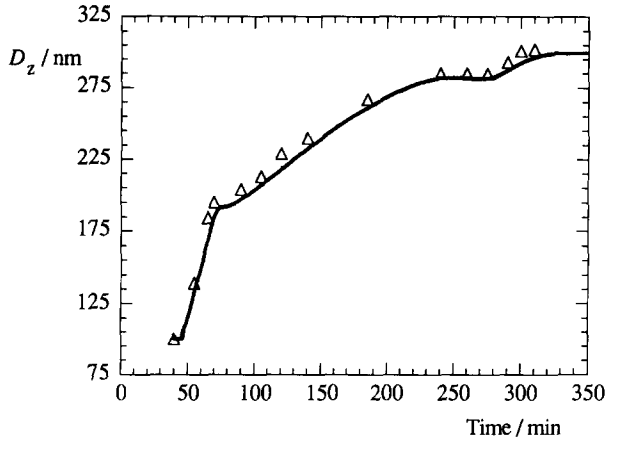

Figure 11 Variation of z-average particle diameter (D_z) with reaction time for preparation of the 4L toughening particles. The solid line is the theoretical curve (see text)

provides strong evidence that the seed particles were grown without significant secondary nucleation. Comparison of the experimental data with the theoretical curves indicates the degree of swelling of the particles (i.e. the cube of the ratio of the experimental to the theoretical particle diameter) by unreacted monomer in each growth stage and shows that the 2L particles are far more extensively swollen than the 3L and 4L particles during the major rubbery layer growth stage. The equation of Morton *et al.*[24] reveals that, other things being equal, the equilibrium concentration of monomer dissolved in a particle should increase as the particle diameter increases, but that the rate of increase with diameter rapidly diminishes as the diameter increases and for particle diameters $\geqslant 100$ nm the equilibrium monomer concentration should be largely insensitive to diameter. Hence, the greater swelling of the 2L particles during the rubbery layer growth stage is not related to differences in particle diameter. A possible explanation is that the much lower rate of polymerization for the 2L particles provides more time for swelling to take place.

The particle size data confirm that the seed particles grew correctly in terms of the increases in size with conversion, but do not provide information on the control of particle morphology. The preparation of well-defined particles with concentric layers is expected to be greatly assisted by crosslinking of the copolymers forming those layers, since this presents a kinetic barrier to thermodynamically driven rearrangements of the different phases within the particles. For preparation of PMMA–PS core–shell particles, Lee and Rudin[25,26] have reported that a well-defined core–shell morphology is obtained when the two polymers are sufficiently crosslinked, and have shown that ALMA is particularly efficient in restricting rearrangements of phases. The crosslinking and graftlinking of the copolymers forming the phases in the toughening particles, therefore, provides conditions which are commensurate with good control of particle morphology. This is confirmed by *Figures 12a–c* which show transmission electron micrographs of thin films cast from dispersions of the toughening particles in solutions of Diakon LG156 in toluene. The rubbery phases appear darker than the glassy phases, thereby clearly revealing the morphology of the particles and, in each case, showing that it is consistent with the

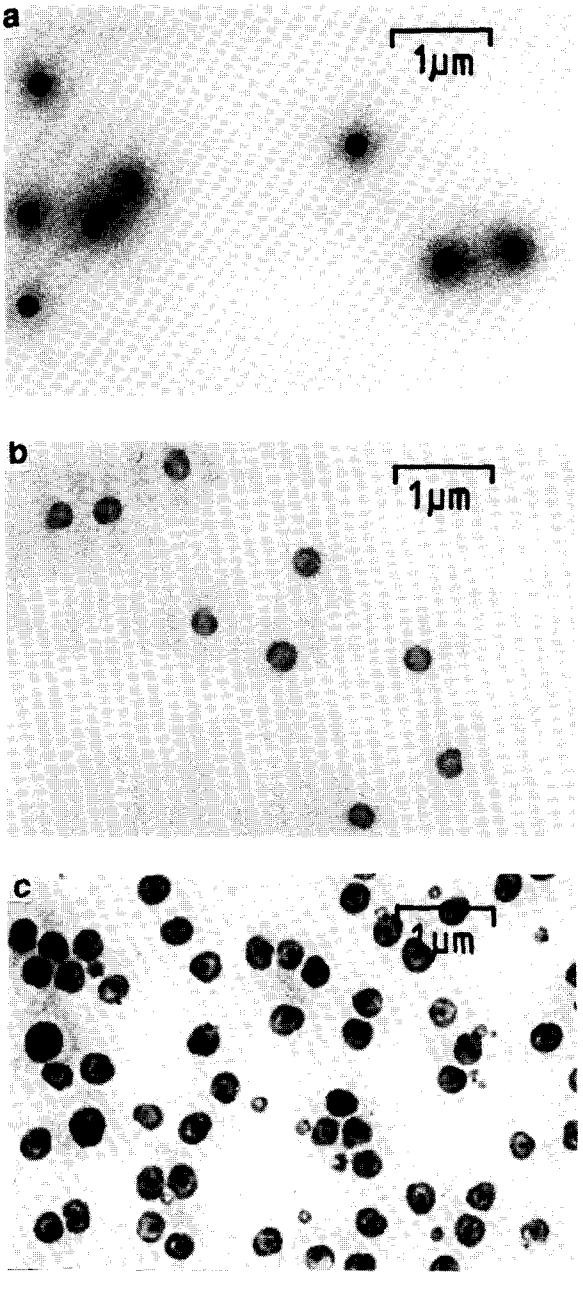

Figure 12 TEM micrographs of films cast from dispersions of the toughening particles in solutions of the matrix PMMA: (a) 2L; (b) 3L; (c) 4L

designed particle structure. The micrographs also show that the particle size distributions are relatively narrow. The contrast between the phases almost certainly is due to degradation (i.e. effective evaporation) of the glassy copolymer[27], leading to higher electron density in the rubbery phases. The outer glassy layers of the particles are not visible because they are of almost identical composition to the matrix PMMA with which they mix.

It is clear from the analytical data, therefore, that the toughening particles had been formed in the manner desired with good control of particle size and morphology. The latex seed particle concentrations were 5.8×10^{16}, 3.7×10^{16} and 4.1×10^{16} particles kg^{-1} for the 2L, 3L and 4L particles, respectively, and correspond to particle surface area concentrations of 1.82×10^3, 1.16×10^3 and 1.29×10^3 $m^2 kg^{-1}$, respectively. The values of these quantities, when considered together, are sufficiently high to expect the seed particles to grow without secondary nucleation[28,29]. Furthermore, the aqueous phase concentrations of surfactant used in the seed stages (0.45 mmol dm^{-3} for the 2L particles and 0.33 mmol dm^{-3} for the 3L and 4L particles) and the levels of surfactant employed to maintain colloidal stability in the growth stages (0.6 and 0.8 wt% for the glassy and rubbery growth stages, respectively) were deliberately chosen to be low in order to limit further the possibility of secondary nucleation[28,30]. Thus, the combined effect of high seed particle concentrations, relatively high particle surface area concentrations and low surfactant concentrations has led to the desired growth of the seed particles. The achieved control of particle morphology, however, must be ascribed to the crosslinking/graftlinking of the layers as they were formed, especially when considering the relatively low instantaneous conversions during the major rubbery layer growth stages which otherwise would have been expected to lead to phase rearrangements within the particles[25,26,31,32].

Morphology and thermal characterization of the RTPMMA materials

The matrix PMMA used for preparation of the blends is in fact poly[(methyl methacrylate)-*co*-(n-butyl acrylate)] with 8.0 mol% BA repeat units[10] and is an 'easy-flow' injection moulding grade manufactured by ICI. Analysis by g.p.c. gives $M_n = 47$ kg mol^{-1}, $M_w = 80$ kg mol^{-1} and $M_w/M_n = 1.7$.

For each of the types of toughening particle, the coagulum produced from the latexes was in the form of aggregates of the primary particles and, typically, had granule sizes in the range 50–400 μm as measured by optical microscopy. In order to establish the quality of re-dispersion of the primary toughening particles achieved by the melt blending process, ultramicrotomed sections were cut from compression-moulded plaques of each of the blends and examined by transmission electron microscopy (TEM). Representative micrographs are shown in *Figures 13a–c*. In addition to revealing that the dispersions of primary toughening particles are good, the micrographs confirm that the morphology and size of the toughening particles is unaffected by the blending process. (The morphology is visible in the same way as for the cast films.) The apparently broader ranges of particle size arise from the fact that individual particles may be cut at any point from their equator to their periphery, and the slight distortions of the particles is a consequence of sectioning the samples at room temperature.

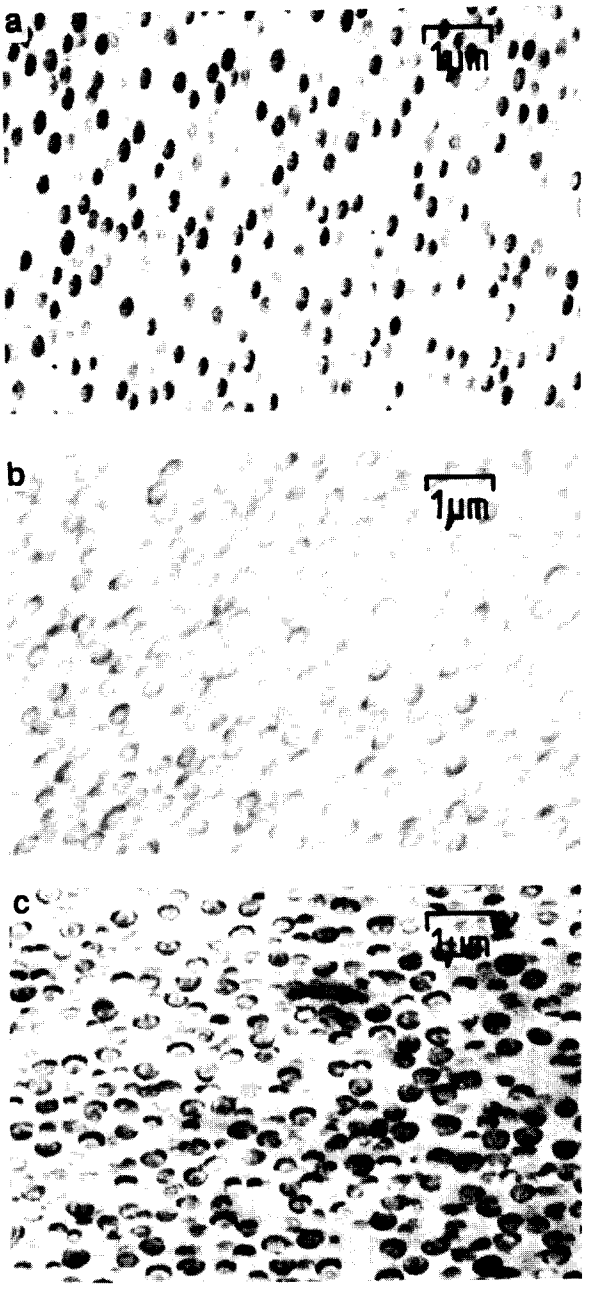

Figure 13 TEM micrographs of ultramicrotomed sections of representative RTPMMA materials: (a) 2L20; (b) 3L22; (c) 4L37

The thermal transitions of the matrix PMMA, the toughening particles and their blends have been investigated using both d.s.c. and d.m.t.a. The glass transition temperatures, T_g^G, of the matrix PMMA and of the glassy phases in the toughening particles and the RTPMMA materials were detectable by d.s.c. and are given in *Table 2*. In contrast, the glass transition temperatures, T_g^R, of the rubbery phases in the toughening particles and the RTPMMA materials were not sufficiently distinct to be measured by d.s.c. Using d.m.t.a., however, it was possible to detect the glass transitions of both the glassy and rubbery phases (*Figure 14*), although the peaks in tan δ associated with the latter were broad and superimposed upon the broad β transition of the matrix PMMA. As a consequence, the peak maxima, and hence T_g^R, are not well defined and are difficult to locate with accuracy. Nevertheless, for

Table 2 T_g^G data from d.s.c. and d.m.t.a. analysis of the toughening particles, the matrix PMMA and the RTPMMA materials

Material	T_g^G (°C)	
	from d.s.c.	from d.m.t.a.
2L particles	101	–
3L particles	101	–
4L particles	101	–
Matrix PMMA	89	107
2L11	93	106
2L20	91	107
2L29	92	107
2L40	96	107
3L11	93	104
3L22	93	104
3L33	94	105
3L40	93	106
4L17	96	106
4L25	93	106
4L37	95	107
4L42	94	107

each of the types of toughening particle and the RTPMMA materials, T_g^R clearly occurs in the range −10 to 0°C. The invariance of T_g^R is expected, since the toughening particles consist of well-defined phases which are crosslinked and can only undergo molecular mixing with the matrix PMMA at the glassy surface. The broad nature of the glass transition of the rubbery phases is consistent with the broad range of copolymer composition arising from the operation of monomer-flooded conditions during the formation of these phases.

The values of T_g^G from d.m.t.a. are presented in *Table 2* for comparison with those from d.s.c., the differences in T_g^G arising from the differences between the two techniques with respect to procedural conditions, temperature detection and transition location. Although d.s.c. gives T_g^Gs which are ~10–15°C lower than those from d.m.t.a., both sets of data are independently self-consistent and show that, within experimental error, T_g^G is invariant with w_p. The T_g^G values obtained by d.s.c. for the RTPMMA materials are intermediate to those of the matrix PMMA and the glassy phases of the toughening particles. D.s.c. is not sufficiently sensitive to resolve the individual transitions of the two or three possible types of glassy phase in the RTPMMA materials (i.e. inner glassy phases in 3L and 4L particles, mixed interfacial regions and 'pure' matrix PMMA). The values of T_g^G may be compared with those predicted from homopolymer T_g values[17]: PMMA, $T_g = 105$°C; poly(ethyl acrylate), $T_g = -24$°C; and poly(n-butyl acrylate), $T_g = -54$°C. Using the Fox equation[18], the T_g^G values for the matrix PMMA and the glassy phases in the toughening particles are predicted to be 79 and 95°C, respectively, whereas linear dependence upon weight fraction composition[17] predicts values of 85 and 99°C, respectively. Thus the T_g^G values obtained by d.s.c. agree most closely with the theoretical predictions.

The value of T_g^R (i.e. −10 to 0°C) may also be compared with the predicted ranges shown in *Figure 7*, which have mean values equal to −36 and −26°C from the Fox equation and the linear relationship, respectively. Hence, even taking into account the fact that d.m.t.a. typically gives T_g values ~10–15°C higher, the T_g^R data

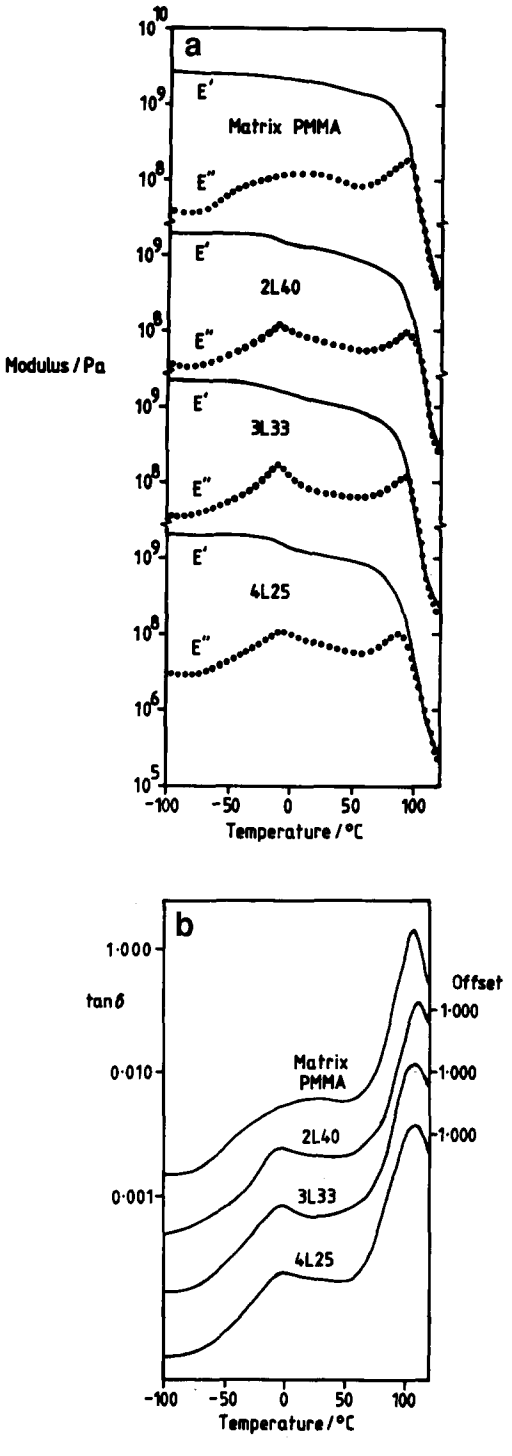

Figure 14 Representative d.m.t.a. spectra for the matrix PMMA and each type of RTPMMA material: (a) storage modulus (E') and loss modulus (E''); (b) tan δ

are slightly higher than expected. This apparent discrepancy may be a consequence of the broad range of rubbery copolymer composition, the difficulty in locating the peak in tan δ and the crosslinking of the rubbery phases, which is not taken into account when calculating the theoretical values.

CONCLUSIONS

Multiple-layer toughening particles comprising two, three and four alternating rubbery and glassy layers have been prepared by sequential emulsion polymerization with good control of particle size and morphology. This

control results from the use of a relatively high seed particle concentration, a low level of surfactant in the growth stages and from crosslinking/graftlinking of the phases. For each of the types of toughening particle, the coagulum produced from the latex was easily disrupted by extrusion blending with the matrix PMMA to give a range of RTPMMA materials containing different levels of well-dispersed primary toughening particles. The toughening particle size and morphology is 'locked-in' by the crosslinking and graftlinking of the phases, and so is retained in the blends. Furthermore, since the rubbery and glassy phases of each of the types of toughening particle were identical in composition, the RTPMMA materials have essentially identical thermal behaviour in terms of the T_gs of the rubbery and glassy phases. Hence, differences in mechanical properties can be confidently assigned to the differences in toughening particle size and/or morphology. The effects of toughening particle size, morphology and level of inclusion upon the mechanical properties of the RTPMMA materials will be discussed in detail in the second paper of this series.

ACKNOWLEDGEMENTS

The authors express their thanks to the Science and Engineering Research Council and to ICI plc for funding the work reported here. The assistance of Pat Hunt, Bill Jung and Mike Chisholm is gratefully acknowledged.

REFERENCES

1 Bucknall, C. B. 'Toughened Plastics', Applied Science, London, 1977
2 Kinloch, A. J. and Young, R. J. 'Fracture Behaviour of Polymers', Applied Science, London, 1983
3 Imperial Chemical Industries Ltd. *BP 965 786*, 1964; *BP 1 093 909*, 1967
4 Rohm and Haas Company. *BP 1 340 025*, 1973; *BP 1 414 187*, 1975; E.I. Du Pont de Nemours and Company. *GB 2 039 496A*, 1979
5 Koppel, D. E. *J. Chem. Phys.* 1972, **57**, 4814
6 Lee, S. P. and Chu, B. *Appl. Phys. Lett.* 1974, **24**, 575
7 Albert, R. and Malone, W. M. *J. Macromol. Sci. Chem.* 1972, **A6**, 347
8 Brandrup, J. and Immergut, E. H. (Eds) 'Polymer Handbook', 3rd Edn, Wiley-Interscience, New York, 1989, Table II, VI, p. 457
9 Brandrup, J. and Immergut, E. H. (Eds) 'Polymer Handbook', 3rd Edn, Wiley-Interscience, New York, 1989, II, p. 153
10 Hunt, P. and Jung, W. personal communcations, 1991
11 Heatley, F., Lovell, P. A. and McDonald, J. *Eur. Polym. J.* in press
12 Wessling, R. A. *J. Appl. Polym. Sci.* 1968, **12**, 309
13 Snuparek, J. and Krska, F. *J. Appl. Polym. Sci.* 1976, **20**, 1753
14 Kaszas, G., Foldes-Berezsnich, T. and Tudos, F. *Eur. Polym. J.* 1984, **20**, 395
15 Brandup, J. and Immergut, E. H. (Eds) 'Polymer Handbook', 3rd Edn, Wiley-Interscience, New York, 1989, Table 3.1, VII, p. 526
16 Calculated using the cohesive energy group contributions of Hoftyzer and Van Krevelen given in: Van Krevelen, D. W. 'Properties of Polymers', 3rd Edn, Elsevier, Amsterdam, 1990, Table 7.1, p. 192
17 Young, R. J. and Lovell, P. A. 'Introduction to Polymers', 2nd Edn, Chapman and Hall, London, 1991, p. 298
18 Fox, T. G. *Bull. Am. Phys. Soc.* 1956, **1**, 123
19 Brandrup, J. and Immergut, E. H. (Eds) 'Polymer Handbook', 3rd Edn, Wiley-Interscience, New York, 1989, VI, p. 213
20 'Diakon-Toughened Grades', ICI information leaflet DN14, 1985
21 Vanderhoff, J. W. in 'Science and Technology of Polymer Colloids' (Eds G. W. Poehlein, R. H. Ottewill and J. W. Goodwin), Vol. 1, Martinus Nijhoff Publishers, The Hague, 1983, p. 8
22 Brandrup, J. and Immergut, E. H. (Eds) 'Polymer Handbook', 3rd Edn, Wiley-Interscience, New York, 1989, II, p. 67
23 Saunders, D. E. J. *PhD Thesis* Victoria University of Manchester, 1990
24 Morton, M., Kaizermann, S. and Altier, M. W. *J. Colloid Sci.* 1954, **9**, 300
25 Lee, S. and Rudin, A. *Makromol. Chem., Rapid Commun.* 1989, **10**, 655
26 Lee, S. and Rudin, A. *Polym. Mater. Sci. Eng.* 1991, **64**, 281
27 Shaffer, O. L. personal communication, 1991
29 Dimonie, V., El-Aasser, M. S., Klein, A. and Vanderhoff, J. W. *J. Polym. Sci., Polym. Chem. Edn* 1984, **22**, 2197
29 Merkel, M. P., Dimonie, V. L., El-Aasser, M. S. and Vanderhoff, J. W. *J. Polym. Sci., Polym. Chem. Edn* 1987, **25**, 1219
30 Brown, R. A., Price, C., Randall, P. D. and Satgurunathan, R. *Polym. Commun.* 1989, **30**, 349
31 Cho, I. and Lee, K.-W. *J. Appl. Polym. Sci.* 1985, **30**, 1903
32 Chen, Y.-C., Dimonie, V. and El-Aasser, M. S. *J. Appl. Polym. Sci.* 1991, **42**, 1049